International Journal of Pharmaceutics 550 (2018) 240–250

Contents lists available at ScienceDirect

International Journal of Pharmaceutics

journal homepage: www.elsevier.com/locate/ijpharm

Dendrimer as a new potential carrier for topical delivery of siRNA: A comparative study of dendriplex vs. lipoplex for delivery of TNF-α siRNA

Palpandi Pandi[a,1], Anjali Jain[a,1], Nagavendra Kommineni[a], Maksim Ionov[b,*], Maria Bryszewska[b], Wahid Khan[a,*]

[a] Department of Pharmaceutics, National Institute of Pharmaceutical Education & Research (NIPER), Hyderabad 500037, India
[b] Department of General Biophysics, Faculty of Biology and Environmental Protection, University of Lodz, Poland

ARTICLE INFO

Keywords:
TNF-α
RNA interference
Dendrimers
Liposomes
Psoriasis

ABSTRACT

Topical delivery of siRNA is challenging task due to complex barrier property of stratum corneum and cationic lipid based carriers have been widely explored for this purpose due to improved permeation through skin. For gene delivery application, dendrimers are considered as efficient carrier due to their cationic nature and well-defined surface groups. However, they are not well explored for topical delivery. This work compares the suitability of PAMAM dendrimer with DOTAP liposome for topical delivery of siRNA against TNF-α. The particle size, zeta potential and entrapment efficiency of dendriplex were 99.80 ± 1.80 nm, 13.40 ± 4.84 mV and 98.72 ± 2.02% whereas for lipoplex were 174.80 ± 0.80 nm, 29.96 ± 0.51 mV and 94.99 ± 5.01% respectively. Both the formulations were stable in serum and in the presence of RNAse. TNF-α is inflammatory cytokine, hence the *in vivo* efficacy of developed formulations was determined using psoriatic plaque model. Results suggested improved phenotypic and histopathological features and reduced levels of IL-6, TNF-α, IL-17 and IL-22 for dendriplex and lipoplex treated groups in comparison to Imiquimod treated group. These findings suggest that dendrimer can be a potential carrier for topical gene delivery.

1. Introduction

RNA interference (RNAi) is the rapidly growing area of research these days due to its targeting at genomic level. Small interfering RNA (siRNA) works on post-transcription phase to downregulate the production of protein and offers significant effects in various disease management and alleviation (Zhou et al., 2014). siRNA does not integrate into DNA thereby avoids the risk of genome modification which is an important factor for regulatory and safety considerations (Sokolova et al., 2007). However, delivery of naked siRNA faces many challenges due to its hydrophilic nature, high molecular weight, and negative charge which does not support cell permeation by passive diffusion mechanisms (Pecot et al., 2011; Jain et al., 2014). Further, naked siRNA is susceptible to enzymatic degradation in plasma followed by renal clearance, resulting inadequate uptake by target cells. The off-target side effects and immune system stimulation are other challenges associated with siRNA therapy (O'Mahony et al., 2012).

For topical applications, skin permeation of macromolecules such as oligonucleotides or proteins has remained a major challenge due to complex barrier property of stratum corneum (SC). Several methods including use of permeation enhancers, iontophoresis, electroporation and acoustic methods (Moser et al., 2001; Barry, 2001) have been employed to deliver sufficient amount of therapeutic agent into the deeper dermal milieu. Vector mediated delivery of siRNA has been a major research interest for various disease conditions and several viral and non-viral vectors have been explored for this purpose. Non-viral vectors offer advantages over the viral delivery systems of being completely biodegradable, less toxic and less immunogenic (Pandi et al., 2017). Non-viral vectors consist of polymeric and lipid based carriers which carry the siRNA either by encapsulation or by charge induced surface interaction. Liposomes (LPM), solid lipid nanoparticles, nanostructured lipid carriers are widely explored for gene delivery application. Lipid vectors are suitable for manipulating surface charge and probe-modification for active targeting, as well as for protecting against degradation by plasma RNases (Akinc et al., 2009; Desai et al., 2013). From among different lipid vectors, LPM are widely explored for topical delivery of various therapeutic agents (Doppalapudi et al., 2017; Bulbake et al., 2017). Polymeric carriers are rigid, stable and offer slow release of siRNA. Another delivery carrier is dendrimer, known for its highly branched structure, uniform dispersion and nano size range

* Corresponding authors at: Department of General Biophysics, Institute of Biophysics, University of Lodz, Pomorska 141/143, 90-236 Lodz, Poland (M. Ionov).
E-mail addresses: maksim.ionov@biol.uni.lodz.pl (M. Ionov), wahid@niperhyd.ac.in (W. Khan).
[1] Authors contributed equally.

https://doi.org/10.1016/j.ijpharm.2018.08.024
Received 17 May 2018; Received in revised form 13 August 2018; Accepted 14 August 2018
Available online 27 August 2018
0378-5173/

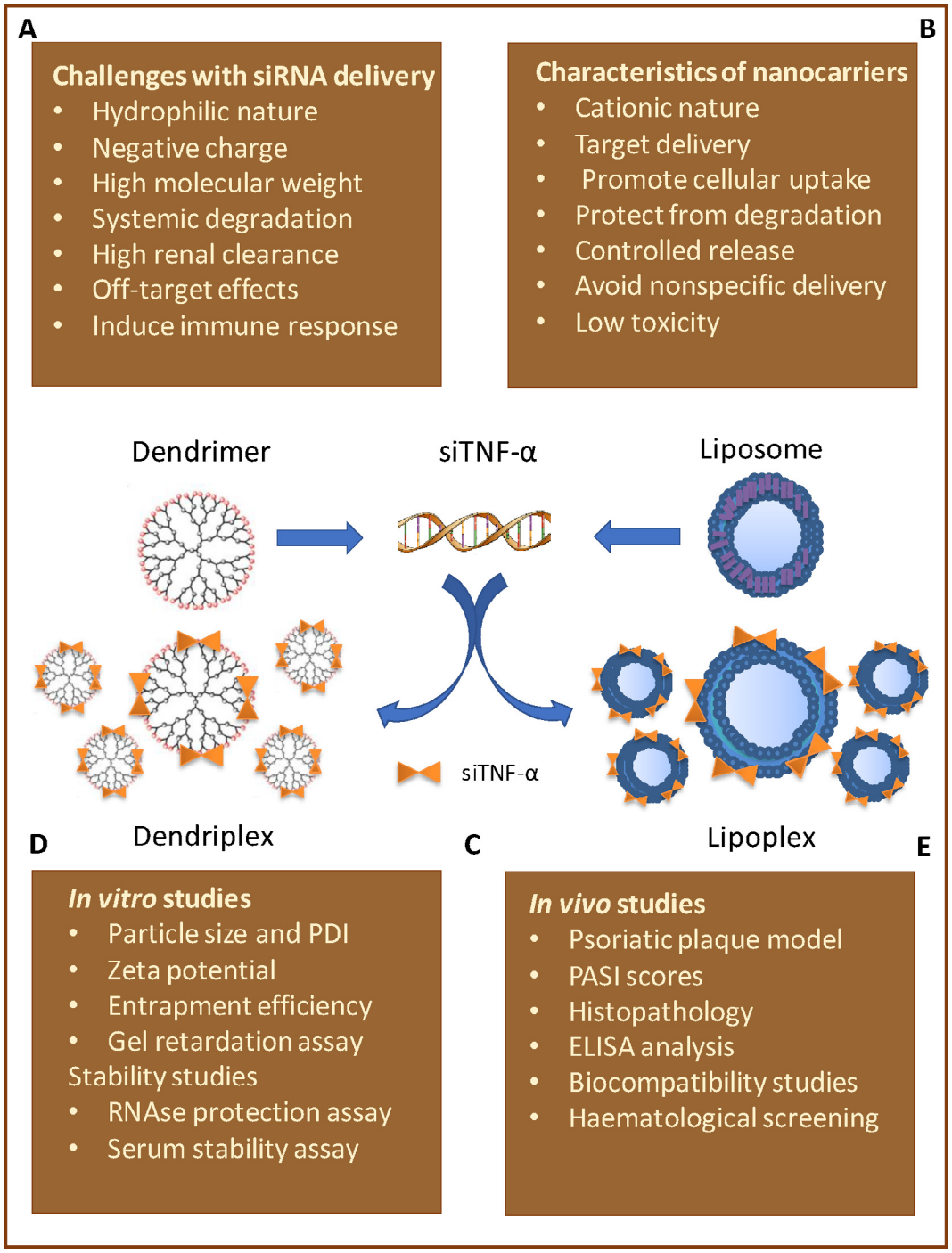

Fig. 1. Schematic presentation describing: (A) challenges with siRNA delivery, (B) characteristics of nanocarriers, (C) formation of dendriplex and lipoplex, (D) *in vitro* studies and stability studies and (E) *in vivo* studies of optimized formulations.

(Uppuluri et al., 1998). For gene delivery application, Polyamidoamine (PAMAM) dendrimers are explored widely due to their narrow molecular weight distribution and easily functionalized amine-terminated surface providing the positive charge for interaction with siRNA (Kang et al., 2005; Jain et al., 2015).

Lipid based formulations are widely used in topical application due to their better penetration through skin layers, however dendrimer based system are relatively less explored for this purpose. Hence, objective of this study is to compare the 1,2-dioleoyl-3-trimethyl ammonium propane (DOTAP) LPM and PAMAM generation-3 (P-G3) dendrimers for the topical delivery of siTNF-α. As siTNF-α is one of the inflammatory mediators which expressed widely in etiology of psoriasis. Hence, the *in vivo* efficacy siTNF-α dendriplex is determined and compared with siTNF-α lipoplex using IMQ induced psoriatic plaque model. Further, hematological toxicity of these carriers were also determined. The schematic layout of this work is given in Fig. 1.

2. Materials and methods

2.1. Materials

Tumor necrosis factor-α siRNA (siTNF-α) was purchased from Dharmacon™, USA. PAMAM dendrimer (P-G3), triton X-100, diethyl pyro carbonate (DEPC) water, ethidium bromide and phosphate buffer

saline (PBS) pH 7.4 were purchased from Sigma-Aldrich, USA. DOTAP (chloride salt) was purchased from Avanti polar lipids, USA. Cholesterol (Chol) was obtained from Lobachem, India. Imiquiad cream (5% w/w imiquimod cream) was obtained from Glenmark Pharmaceuticals, India. Betnovate® (betamethasone valerate ointment, 0.1% w/w) was procured from Glaxo SmithKline Pharmaceutical Limited, India. Chloroform was obtained from Merck Pvt. Ltd. India. Formaldehyde was obtained from HiMedia laboratories, India. ELISA kits for interleukin-17 (IL-17), interleukin-22 (IL-22), interleukin-6 (IL-6) and tumor necrosis factor-α (TNF-α) were purchased from R&D Systems, USA. Tris EDTA buffer (TE) (10X and 1X), RNAse free water, agarose gel and bromophenol blue dye were purchased from Cleaver scientific private limited, UK. Heparin was obtained from Gland Pharma Limited, India. Bromo phenol blue dye was obtained from Cleaver Scientific Private Limited, India. Quanti-iT™ Ribogreen® reagent and RNA standard stock were purchased from Molecular probes, Life technologies™, Invitrogen Bioservices Pvt Ltd. (Bangalore, India). Dulbecco's modified eagle's medium (DMEM) was purchased from Invitrogen (Massachusetts, USA).

2.2. Formulations development

2.2.1. Preparation of P-G3 dendriplex

Dendrimer/siRNA complexes were formed using reported method with slight modification (Ionov et al., 2015). The equal volumes of siRNA and dendrimer solutions were mixed at concentrations giving the desired N/P molar ratio. The mixture was incubated for 10 min at 22 °C. 10 mM/L Na-phosphate buffer, pH 7.4, was used for preparation of dendriplex.

2.2.2. Preparation of DOTAP lipoplex

LPM were prepared using reported method (Podesta and Kostarelos, 2009) by dissolving Chol and DOTAP lipid in chloroform at molar ratio 1:1. A dry thin lipid film was prepared in a round bottom flask using a rotary evaporator (Heidolph, Heidolph Instruments GmbH & Co. Germany). After the formation of thin film, the hydration was carried out by RNAse free DEPC treated water at a temperature of 37 °C to form multilamellar vesicles (MLV). The so formed MLVs were sonicated using probe sonicator (Sonics, Vibra Cell, USA) to acquire unilamellar liposomal dispersion. Finally, the siRNA buffered solution was added to liposomal dispersion at desired siRNA/lipid (N/P) molar ratio and incubated for 30 min to allow stable complexes to be formed.

2.3. Analytical method for siRNA

Ribogreen assay was performed for quantitative determination of siTNF-α complexed with LPM and P-G3 dendrimer (Sato et al., 2012; Jones et al., 1998). For high range calibration curve, Quanti-iT™ Ribogreen reagent was diluted 200 folds using Tris-EDTA buffer (TE) (10 mM Tris-HCl, 1 mM EDTA, pH 7.5) and 100 µL of the reagent solution was added to microplate wells containing 100 µL ribosomal RNA in TE. For the low range assay, Quanti-iT™ Ribogreen reagent was diluted 2000 folds with TE, and 100 µL of the reagent solution was added to microplate wells containing 100 µL of ribosomal RNA in TE. The excitation maximum for Quant-iT™ RiboGreen® reagent bound to RNA is 500 nm and the emission maximum is 525 nm.

2.4. Gel retardation and integrity assay

Agarose gel electrophoresis was used to study formation of dendriplex and lipoplex of siTNF-α and to determine the protection of siRNA complex from ribonucleolytic degradation (Du et al., 2012). For comparison, plain siTNF-α was used for this study. The prepared dendriplexes and lipoplexes were mixed with bromophenol dye at 1:6 dilution and added to different wells. The gel electrophoresis was performed for 35 min at 60 mA in a 3% agarose gel containing ethidium bromide. After electrophoresis, the gel was visualized using UV transilluminator (Gel Doc™ XR + system, Biorad laboratories, Inc., USA) at a wavelength of 365 nm and a digital photograph of the stained gel was obtained.

2.5. Characterization of formulations

2.5.1. Particle size and zeta potential

The particle size and size distribution of complexes were measured by the dynamic light scattering technique using a Zetasizer Nano-ZS in DTS0012 plastic cells (Malvern instrument Ltd. UK). Particle size was measured from the average of 10 cycles at 25 °C. Particle surface charge was also measured by Zetasizer. Capillary plastic cell DTS1061 was used to measure the electrophoretic mobility of the samples in an applied electric field. For each sample, 10–15 measurements of zeta potential were collected and average was determined.

2.5.2. Entrapment efficiency

Ribogreen assay was performed to determine the encapsulation efficiency of siRNA complexed with LPM and dendrimers using reported method with slight modification (Zhang et al., 2010). Low range and high range calibration curve were prepared (analytical method section) and used to calculate entrapment efficiency. Dendriplex with N/P ratio of 2:1 and lipoplex with N/P ratio of 110:1 were prepared using PBS pH 7.4 and centrifuged in 15,000 rpm for 15 min. Supernatants were collected, diluted with TE buffer and analyzed using spectrofluorometer (excitation 500 nm, emission 525 nm). Entrapment efficiency was calculated using formula given below.

$$\text{Entrapment efficiency}\,\% = \frac{\text{Encapsulate siRNA concentration}}{\text{Initial siRNA concentration}} \times 100$$

2.6. Stability studies

2.6.1. RNAse protection assay

RNAse protection assay was performed (Kim et al., 2010; Somiya et al., 2015) to determine the protective effect of P-G3 and lipoplex against RNAse mediated degradation. Briefly, optimized dendriplex, lipoplex and naked siRNA were treated with RNAse (1.25 µg/mL) for 30 min at 37 °C. After 30 mins of incubation, the samples were kept on an ice bath for 5 min to arrest the reaction followed by addition of Triton X-100 (1% v/v) for lipoplex and heparin for dendriplex. Migration of siRNA was observed using gel electrophoresis.

2.6.2. Serum stability assay

The serum stability assay was performed to study the stability of siTNF-α loaded dendriplex and lipoplex in serum (Koide et al., 2016). The optimized dendriplex and lipoplex were incubated with equal volume of DMEM supplemented with 10% of FBS at 37 °C. At each time interval (0, 0.5, 1, 2, 4, 9, 12 and 24 h), 30 µL sample was collected and stored in −20 °C until gel electrophoresis was performed. Before gel electrophoresis, the siRNA was released from dendriplex by addition of heparin and from lipoplex by addition of Triton X.

2.7. Skin compliance studies

Skin compliance study was performed on healthy BALB/c mice (Jain et al., 2017). Briefly, different formulations were applied on the dorsal skin of mice for 6 consecutive days. On the 7th day of the experiment animals were sacrificed and skin samples were collected and fixed in 10% v/v formalin solution. Histopathology examination was performed for collected skin samples.

2.8. Hematological screening

Blood samples from different animals were withdrawn at the end of skin compliance study for hematological screening. The samples were

Table 1
Different treatment groups for anti-psoriatic efficacy in IMQ induced psoriatic plaque model.

Days	Normal Healthy untreated mice	IMQ Psoriasis induced untreated mice	Betamethasone Psoriasis induced mice + Betamethasone treatment	siTNF-α Psoriasis induced mice + siTNF-α solution treatment	P-G3 blank Psoriasis induced mice + P-G3 blank treatment	P-G3 + siTNF-α Psoriasis induced mice + (P-G3 + siTNF-α) treatment	LPM blank Psoriasis induced mice + LPM blank treatment	LPM + siTNF-α Psoriasis induced mice + (LPM + siTNF-α) treatment
Day 1	–	IMQ	IMQ	IMQ	IMQ	IMQ	IMQ	IMQ
Day 2	–	IMQ	IMQ	IMQ	IMQ	IMQ	IMQ	IMQ
Day 3	–	IMQ	IMQ + Betamethasone	IMQ + siTNF-α solution	IMQ + P-G3 blank solution	IMQ + (P-G3 + siTNF-α)	IMQ + LPM blank	IMQ + (LPM + siTNF-α)
Day 4	–	IMQ	IMQ + Betamethasone	IMQ + siTNF-α solution	IMQ + P-G3 blank solution	IMQ + (P-G3 + siTNF-α)	IMQ + LPM blank	IMQ + (LPM + siTNF-α)
Day 5	–	IMQ	IMQ + Betamethasone	IMQ + siTNF-α solution	IMQ + P-G3 blank solution	IMQ + (P-G3 + siTNF-α)	IMQ + LPM blank	IMQ + (LPM + siTNF-α)
Day 6	–	IMQ	IMQ + Betamethasone	IMQ + siTNF-α solution	IMQ + P-G3 blank solution	IMQ + (P-G3 + siTNF-α)	IMQ + LPM blank	IMQ + (LPM + siTNF-α)
Day 7	Sacrifice, measurement of ear thickness, skin collection for histopathology and ELISA							

suspended in heparin solution. Red blood cells, white blood cell count, hemoglobin, hematocrit, platelet count and various parameters were analyzed using blood analyzer (Siemens Advia 2120 hematology analyzer, India) (Chen et al., 2004).

2.9. Efficacy studies

2.9.1. IMQ-induced psoriatic plaque model

The IMQ induced psoriatic plaque model was developed as described earlier (van der Fits et al., 2009) and the anti-psoriatic activity of the optimized formulation was assessed (Jain et al., 2016). To induce the psoriatic lesions, marketed imiquad cream (Imiquimod cream, 5% w/w, Glenmark Pharmaceuticals Ltd., India) was applied topically (2 cm^2 area) to the shaven dorsal region and left ear of BALB/c mice at a dose of 62.5 mg/day for 6 days. Betamethasone® (0.1% w/w, GSK Pharmaceuticals Ltd., India) was used as a positive control. Table 1 represents study protocol for IMQ induced psoriatic plaque model. Dendriplex, lipoplex formulations of siTNF-α and siTNF-α alone were tested. In this study, formulations containing 0.5 μM dose of siTNF-α were used. Application of different treatments on the respective animal groups was started on the 3rd day and continued until the 6th day of experiment. Animals were sacrificed on the 7th day and spleen weights of all the animals were recorded. Skin samples of all animals were collected and fixed in 10% formalin solution for histopathological examination. Skin samples were also stored at −80 °C for determination of inflammatory cytokines level (Sun et al., 2017).

2.9.2. Scoring severity of skin inflammation

Psoriasis area severity index (PASI) scores were used to evaluate the severity of psoriatic lesions characterized by three major clinical signs: i.e. erythema (redness), skin thickness (induration) and scaling (desquamation) (Fadzil et al., 2009). The scores were assigned on a 4-point scale where, 0 indicates none; 1-slight; 2-moderate; 3-marked; 4-very marked. These scores were plotted with various groups on x-axis and PASI score (0–4) on y-axis.

2.9.3. Histopathology

Histopathological examination was performed to determine the pathological changes in skin occurred during psoriatic model development (De Rosa and Mignogna, 2007). Formalin fixed skin samples were embedded in paraffin and stained with hematoxylin and eosin (H&E stain). Sections were analyzed under microscope (Eclipse Ts2-FL microscope, USA).

2.9.4. Determination of cytokines levels

ELISA experiments were performed on mice skin collected from different treatment groups (Doppalapudi et al., 2017). Skin tissues were homogenized in an extraction buffer (10 mM Tris pH 7.4, 150 mM NaCl, 1% Triton X- 100) using a tissue homogenizer (Remi electrokinetic, Ltd., India) at 3000 rpm for 5 min. The homogenates were centrifuged at 13,000 rpm for 15 min at 4 °C, and the collected supernatants were stored at −80 °C until analyzed. Levels of IL-17, IL-22, IL-6 and TNF-α were measured using respective ELISA kits as per manufacturer's protocol.

2.10. Statistical analysis

The statistical analysis was performed using GraphPad Prism 6.0 (version 6.05, GraphPad software, Inc., USA). The obtained data was analysed utilizing one-way ANOVA followed by Bonferroni's multiple comparisons test, where $p < 0.05$ was considered statistically significant.

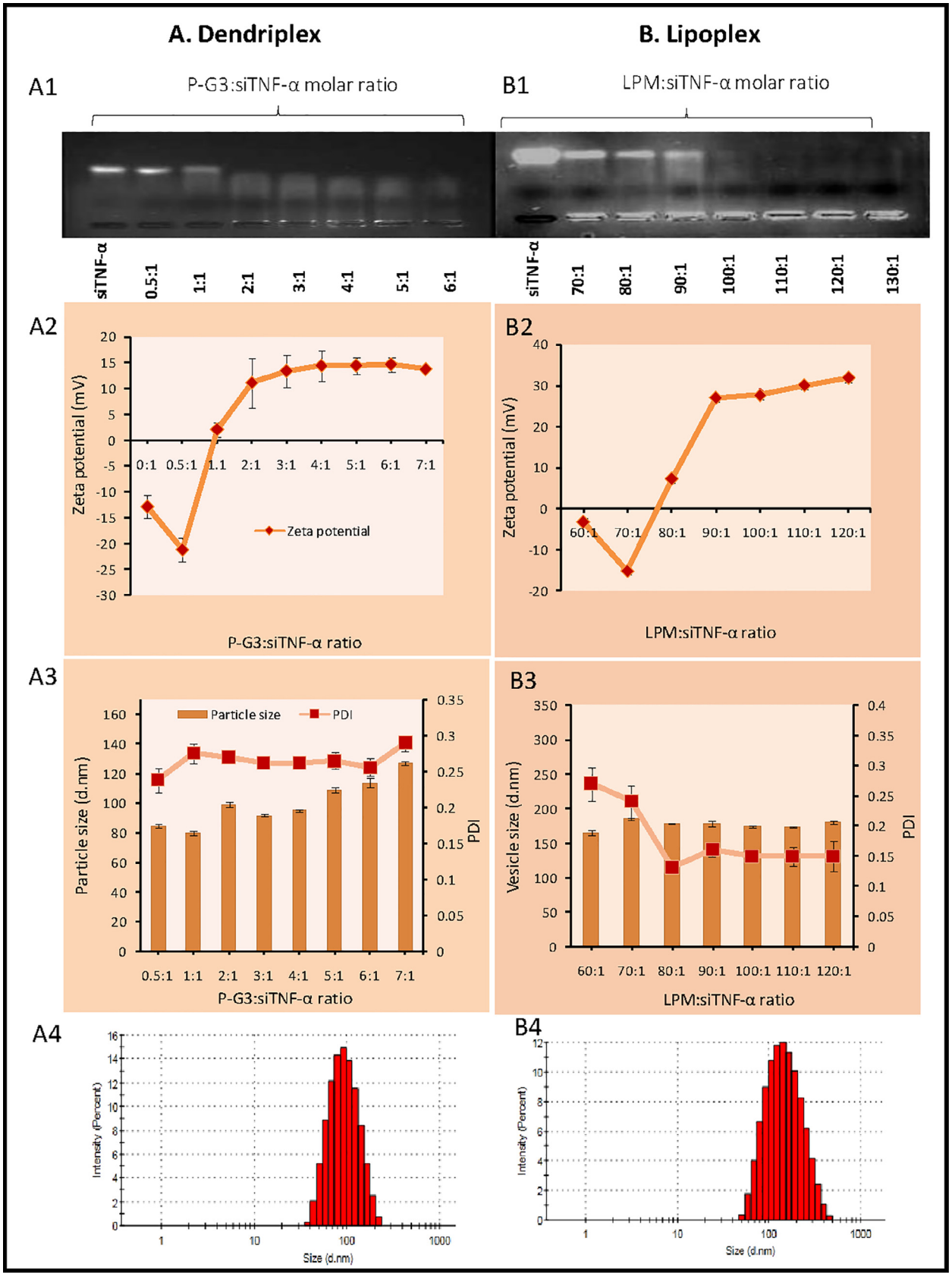

Fig. 2. Formation and characterization of dendriplex and lipoplex. For dendriplex of P-G3 and siTNF-α: (A1) Gel electropherogram of dendriplex, (A2) zeta potential of dendriplexes with different molar ratio, (A3) particle size and PDI of dendriplexes with different molar ratio, (A4) mean particle size of optimized dendriplex formulation. For lipoplex of DOTAP LPM and siTNF-α: (B1) Gel electropherogram of lipoplex, (B2) zeta potential of dendriplexes with different molar ratio, (B3) particle size and PDI of lipoplexes with different molar ratio, (B4) mean particle size of optimized lipoplex formulation.

3. Results

3.1. Formulation development and complexation

The P-G3 dendriplex and lipoplex with various N/P ratios were prepared and complexation pattern of dendrimer and LPM with siTNF-α was studied using Agarose gel electrophores. Fig. 2A1 and B1 represents electropherograms of dendriplexes and lipoplexes with migration pattern of siTNF-α at different N/P ratio and molar ratio. Complexation results in the electro-neutralization of the negative charge of siTNF-α (Tang et al., 2012). For plain siTNF-α solution, a clear band was observed (lane 1) on each electropherogram. Free siRNA and non-complexed siRNA moved in gel electropherogram which can be observed by presence of distinct band while dendriplex/lipoplex with optimum N/P ratios did not show any band due to electro-neutralization of siTNF-α. For P-G3 dendrimer and lipoplex, complexation was observed at 2:1 N/P ratio and 110:1 molar ratio respectively. Further increase in N/P ratio or molar ratio did not give any band which indicated formation of stable complex.

3.2. Characterization of dendriplexes and lipoplexes

The P-G3 dendriplex and lipoplex with various N/P ratios were characterized for zeta potential, mean particle size and PDI. In zeta potential experiment, the N/P ratio of dendriplex was varied from 0.5:1 to 7:1 and change in zeta potential was plotted against N/P ratio. Addition of P-G3 dendriplex to siTNF-α changed zeta potential from −21.20 to 14.66 mV (Fig. 2A2). Zeta potential was found to be increased with increasing the quantity of dendrimer and stabilized after reaching the complexation point. Similarly, the molar ratio of lipoplex was varied from 60:1 to 120:1 which showed the change in zeta potential from −15.15 to 31.75 mV (Fig. 2B2).

For particle size determination of P-G3 dendriplex, N/P ratio was varied from 0.5:1 to 7:1 and particle size increased gradually with increase in N/P ratio (Fig. 2A3). The mean particle size of all the dendriplexes were found to be below 130 nm and the PDI was less than 0.3. A dendriplex with optimized N/P ratio of 2:1 resulted in particle size 99.80 ± 1.80 nm (Fig. 2A4). For lipoplex preparation, the blank LPM of particle size 178.01 ± 5.26 nm was obtained by thin film hydration method. LPM were incubated with siTNF-α at different molar ratio (from 60:1 to 120:1 molar ratio of LPM to siTNF-α) to form lipoplex. For all lipoplexes, particle size and PDI were below 200 nm and 0.3 respectively (Fig. 2B3). An optimized molar ratio of 110:1 of LPM and siTNF-α resulted in average particle size of 174.80 ± 0.80 nm (Fig. 2B4).

The entrapment efficiency of complexed siTNF-α was measured by Quant-iT™ RiboGreen® RNA reagent assay. Entrapment efficiency of P-G3 dendriplex and lipoplex were found to be 98.72 ± 2.02% and 94.99 ± 5.01% respectively. A summary of mean particle size, zeta potential and entrapment efficiency of optimized dendriplex and lipoplex is shown in Table 2.

3.3. Stability studies

3.3.1. RNAse protection assay

RNase protection assay was performed to evaluate the stability of dendriplex and lipoplex in the presence of RNAse enzyme. Fig. 3A represented RNAse protection assay for P-G3 dendriplex, and lipoplex. In Fig. 3A1 first lane shows migration of non-complexed siTNF-α. The second lane shows non-migration of siTNF-α previously incubated with RNase due to degradation of siRNA by RNAse. Third lane represents the P-G3 dendriplex formulation with no band due to formation of complex between dendrimer. The fourth lane contains the dendriplex along with heparin and RNAse and this lane was observed with the appearance of band. The dendriplex protected siRNA from degradation by RNAse, when the heparin was added before loading the sample to agarose gel, heparin released the siRNA from dendriplex and the band was observed due to migration of siRNA on gel. In lipoplex, Triton X-100 was used to release the siRNA from lipoplex and the similar pattern (as observed for P-G3 dendriplex) was observed (Fig. 3A2). These observations indicate that both dendrimer and LPM can protect siRNA from RNAse induced degradation.

3.3.2. Serum stability assay

Serum stability assay was performed to analyze the stability of dendriplex and lipoplex formulations in the presence of serum proteins. Serum stability was tested by incubating formulations with 10% FBS. Fig. 3B showed serum stability assay for P-G3 dendriplex and lipoplex. Naked siRNA was found to be intact till 3 h but degraded completely after 6 h (Fig. 3B1). However, siRNA loaded P-G3 dendriplex (Fig. 3B2) and lipoplex (Fig. 3B3), complexes were stable till 24 h with the appearance of clear bands. Hence it was evidenced that the dendriplex and lipoplex provided protection to siTNF-α from the serum nuclease degradation.

3.4. Skin compliance studies

Skin compliance study was performed on healthy mice skin to determine the skin compatibility of siTNF-α and nanocarriers and to observe any morphological or histopathological changes in mice skin with the selected dose of siTNF-α for efficacy study by H&E staining of treated samples (Fig. 4). The mice epidermis treated with P-G3 dendriplex and lipoplex remained intact with no obvious change in histopathological features. Further, no inflammatory symptoms were observed in skin exposed to the different formulation in comparison to normal skin, indicating that they are safe for topical application.

3.5. Hematological screening

Hemotoxicity of topically applied P-G3 dendriplex and lipoplex were screened. The repeated formulation dose study revealed no significant changes in hematological parameters as compared to normal group as described in Table 3.

3.6. Efficacy studies

3.6.1. IMQ-induced psoriatic plaque model

IMQ induced psoriasis was developed in BALB/c mice to investigate the efficacy of topical siTNF-α in psoriasis. The symptoms closely resemble human plaque-type psoriasis with respect to erythema (hyperkeratosis with parakeratosis), skin thickening, scaling and epidermal alteration (acanthosis).

3.6.2. Scoring severity of skin inflammation

PASI scoring was done on 6th day of IMQ induced psoriatic plaque model. IMQ group showed severe erythema (Fig. 5A), scaling (Fig. 5B)

Table 2
Feature of optimized P-G3 dendriplex and lipoplex.

Optimized N/P ratio	Particle size (nm)	PDI	Zeta potential (mV)	Entrapment efficiency (%)
P-G3 dendriplex (2:1)	99.80 ± 1.80	0.26 ± 0.09	13.40 ± 4.84	98.72 ± 2.02
Lipoplex (110:1)	174.80 ± 0.80	0.15 ± 0.01	29.96 ± 0.51	94.99 ± 5.01

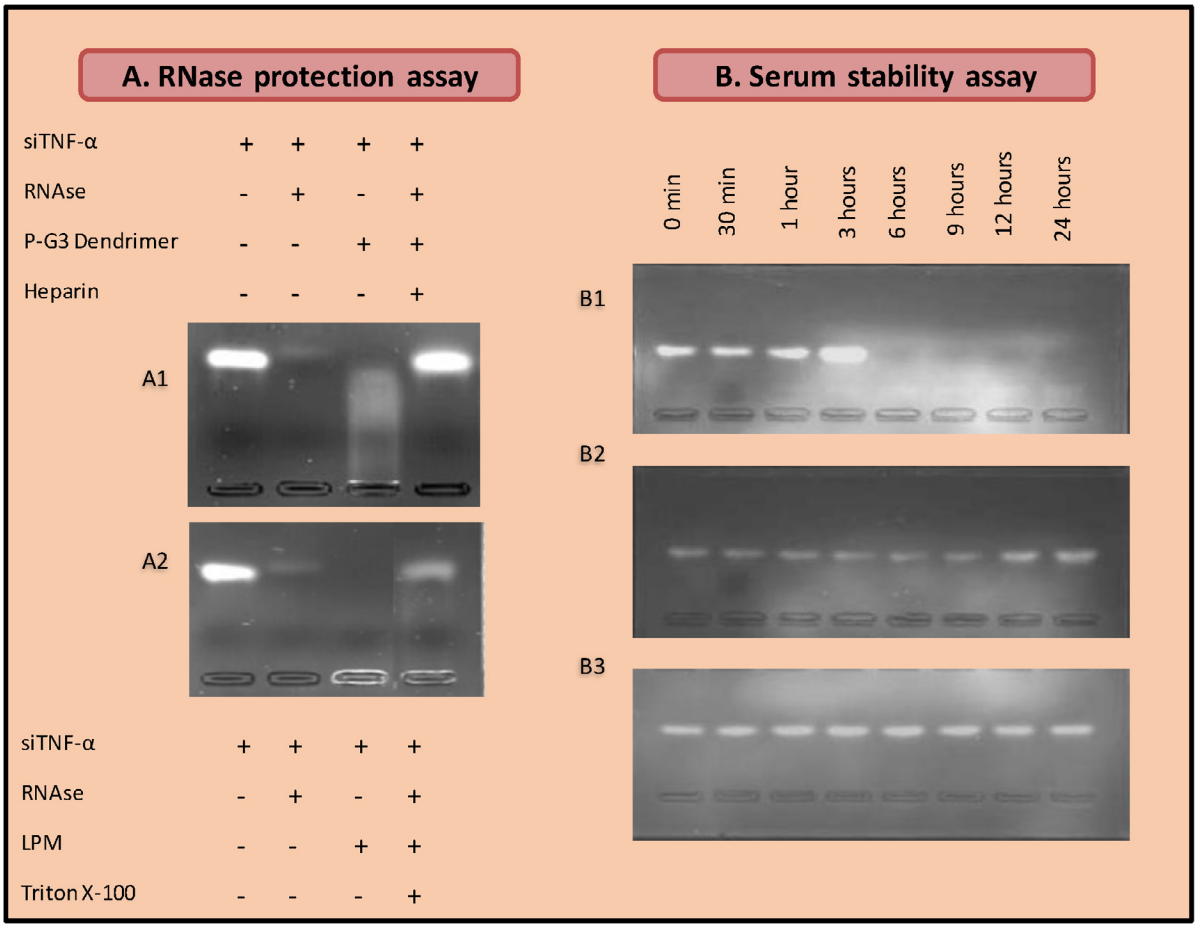

Fig. 3. Stability studies of dendriplex and lipoplex. (A) RNAse protection assay (A1) P-G3 dendriplex (A2) lipoplex. The first lane contains non-complexed siTNF-α resulting migration band. The second lane contains siTNF-α incubated with RNAse. Third lane contains dendriplex/lipoplex. The fourth lane contains siTNF-α, RNAse and heparin/triton X-100 resulting migration band. (B) Serum stability studies were performed in DMEM contains 10% FBS. (B1) Plain siTNF-α, (B2) P-G3 dendriplex and (B3) lipoplex.

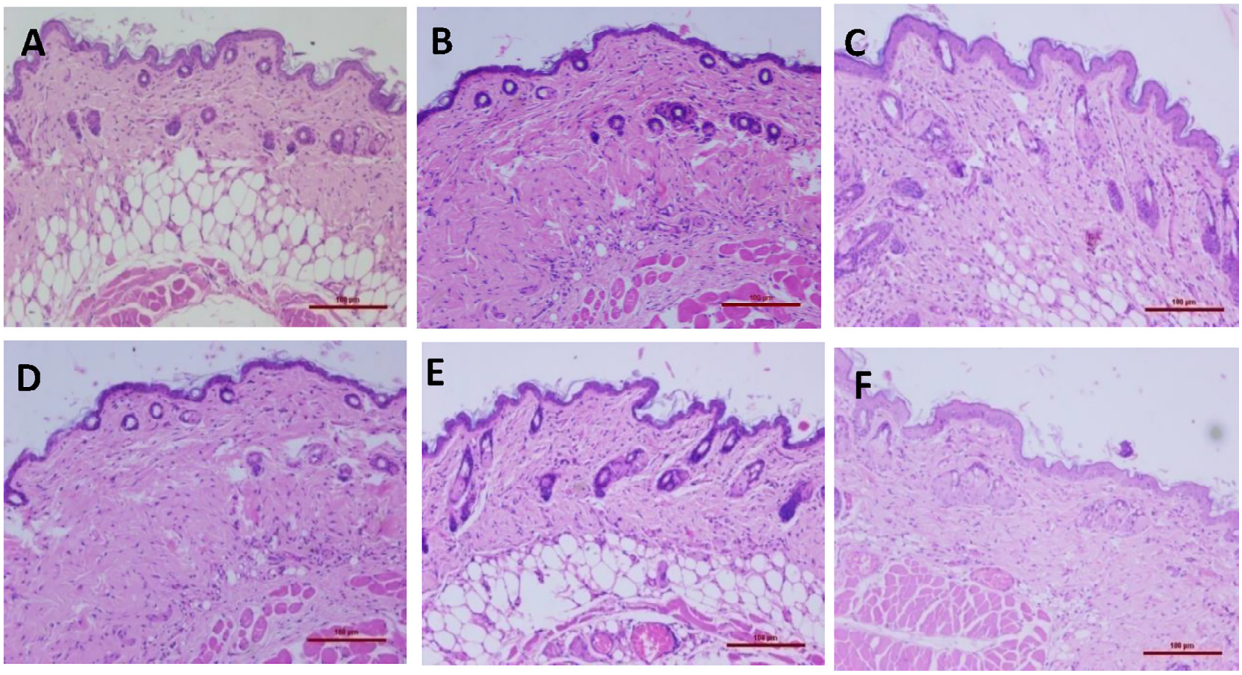

Fig. 4. *In vivo* skin compliance studies. (A) Normal, (B) plain siTNF-α group, (C) blank P-G3 group; (D) P-G3 + siTNF-α group, (E) blank LPM group, (F) LPM + siTNF-α group.

Table 3
Hematological screening for different formulation of siTNF-α.

Blood parameters		Animal groups					
		Normal	Plain siTNF-α	P-G3 blank	P-G3 + siTNF-α	LPM blank	LPM + siTNF-α
WBCP	$\times 10^3$ cells/μL	9.67 ± 1.22	10.20 ± 3.91	11.19 ± 2.34	9.12 ± 4.10	9.83 ± 3.07	8.18 ± 1.16
WBCB	$\times 10^3$ cells/μL	10.09 ± 0.78	9.65 ± 4.51	10.01 ± 2.34	8.14 ± 3.57	8.43 ± 3.07	9.10 ± 0.95
RBC	$\times 10^6$ cells/μL	8.65 ± 1.24	8.33 ± 0.36	9.03 ± 0.74	8.38 ± 0.52	8.70 ± 0.74	8.51 ± 1.02
HGB	g/dL	113.24 ± 2.67	14.26 ± 0.70	13.27 ± 1.27	13.77 ± 1.20	13.77 ± 0.81	12.88 ± 1.57
HCT	%	445.12 ± 4.56	44.60 ± 2.62	45.57 ± 1.40	44.70 ± 1.96	44.97 ± 3.03	44.45 ± 4.79
MCV	fL	552.26 ± 5.46	53.50 ± 0.87	50.63 ± 2.64	53.33 ± 1.02	51.67 ± 1.20	52.38 ± 1.93
MCH	Pg	115.30 ± 1.24	17.07 ± 0.11	14.67 ± 0.47	16.43 ± 0.40	15.87 ± 0.63	15.20 ± 0.80
MCHC	g/dL	229.30 ± 2.45	31.93 ± 0.30	29.03 ± 1.95	30.80 ± 1.30	30.73 ± 1.15	28.98 ± 0.78
CHCM	g/dL	229.98 ± 3.46	31.00 ± 0.78	28.43 ± 1.68	30.30 ± 1.60	29.70 ± 0.79	28.70 ± 0.58
RDW	%	115.30 ± 2.15	14.67 ± 1.45	16.63 ± 1.97	14.83 ± 1.56	14.27 ± 0.90	16.40 ± 2.62
HDW	g/dL	2.43 ± 0.14	2.14 ± 0.21	2.01 ± 0.14	1.89 ± 0.24	1.83 ± 0.05	2.09 ± 0.15
PLT	$\times 10^3$ cells/μL	143 ± 17.45	138 ± 2.82	309 ± 34.64	165 ± 24.58	255 ± 24.04	278 ± 16.86
MPV	fL	335.12 ± 3.35	34.07 ± 5.23	30.10 ± 0.35	32.87 ± 10.28	32.70 ± 3.10	31.78 ± 0.80

Data as mean ± SE (n = 3).
Abbreviations: WBCP – White blood cell count perox, WBCB – White blood cell count baso, HGB – Hemoglobin, HCT – Hematocrit, MCV – Mean corpuscular volume, MCH – Mean corpuscular hemoglobin, MCHC – Mean corpuscular hemoglobin concentration, CHCM – Cell hemoglobin concentration mean, RDW – Red cell distribution width, HDW – Hemoglobin distribution width, PLT – Platelets, MPV – Mean platelet volume.

and skin thickening (Fig. 5C) with a score in range of 2–4 indicating the induction of psoriasis. PASI scores were significantly high in IMQ group in comparison to normal group. Treatment with plain siTNF-α, blank P-G3 and blank LPM groups did not show any improvement in the symptoms. Treatment groups P-G3 + siTNF-α (PASI score 1.25) and LPM + siTNF-α (PASI score 1.6) resulted in reduction of erythema in comparison to IMQ group (PASI score 2.5). Similarly, scaling was reduced in P-G3 + siTNF-α (PASI score 1.5) and LPM + siTNF-α (PASI score 1.4) groups in comparison to IMQ group (PASI score 2.7). Skin thickness for P-G3 + siTNF-α (PASI score 2) and LPM + siTNF-α (PASI score 1.0) was also reduced in comparison to IMQ group (PASI score 2.4). Spleen weight to body weight ratios were determined where negative control showed a higher ratio in comparison to treatment groups. (Fig. 5D).

3.6.3. Histopathology

Histopathology and phenotypic images of different control and treatment groups during IMQ induced psoriatic plaque models are given in Fig. 6. Normal skin contained epidermis and dermis layers. IMQ control exhibited thickening of stratum corneum (hyperkeratosis),

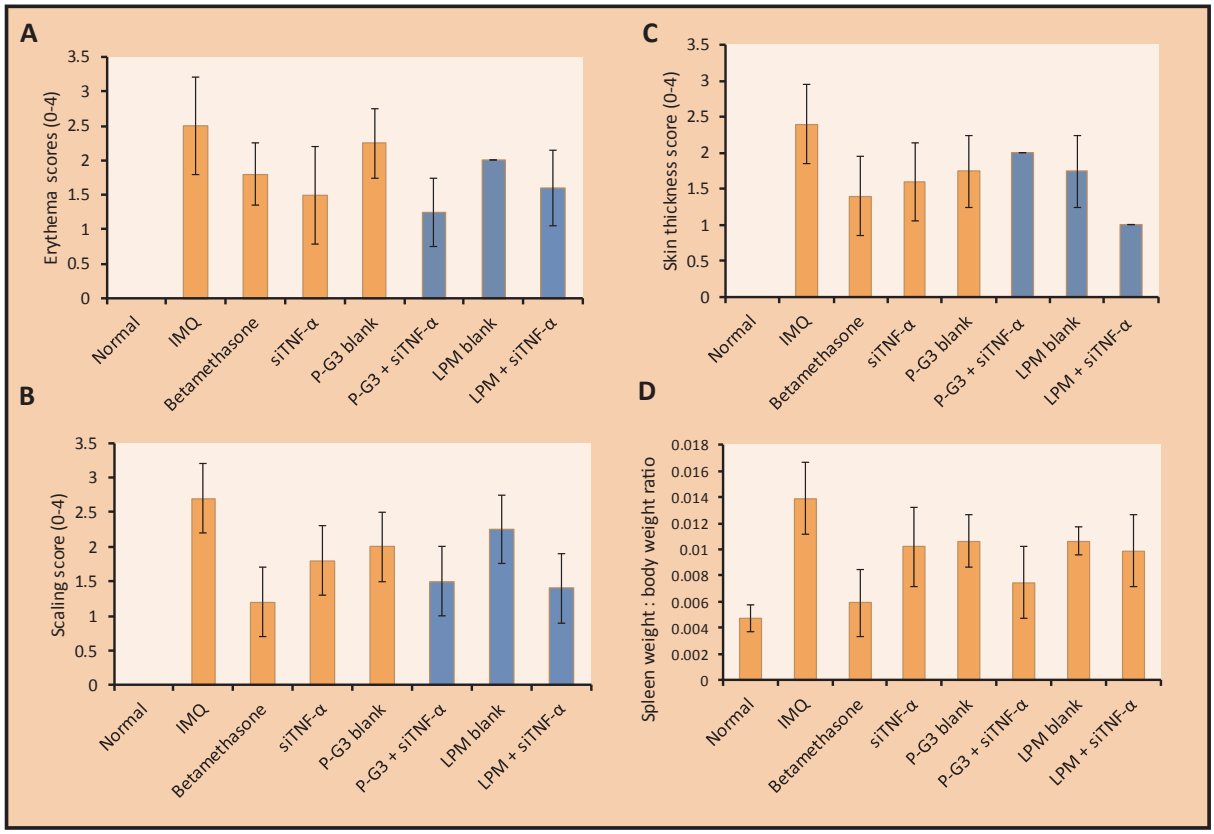

Fig. 5. PASI scoring and spleen weight to body weight assessment during IMQ induced psoriatic plaque model. (A) PASI scores for erythema, (B) PASI scores for scaling, (C) PASI scores for skin thickening, (D) spleen weight to body weight ratio for different study groups.

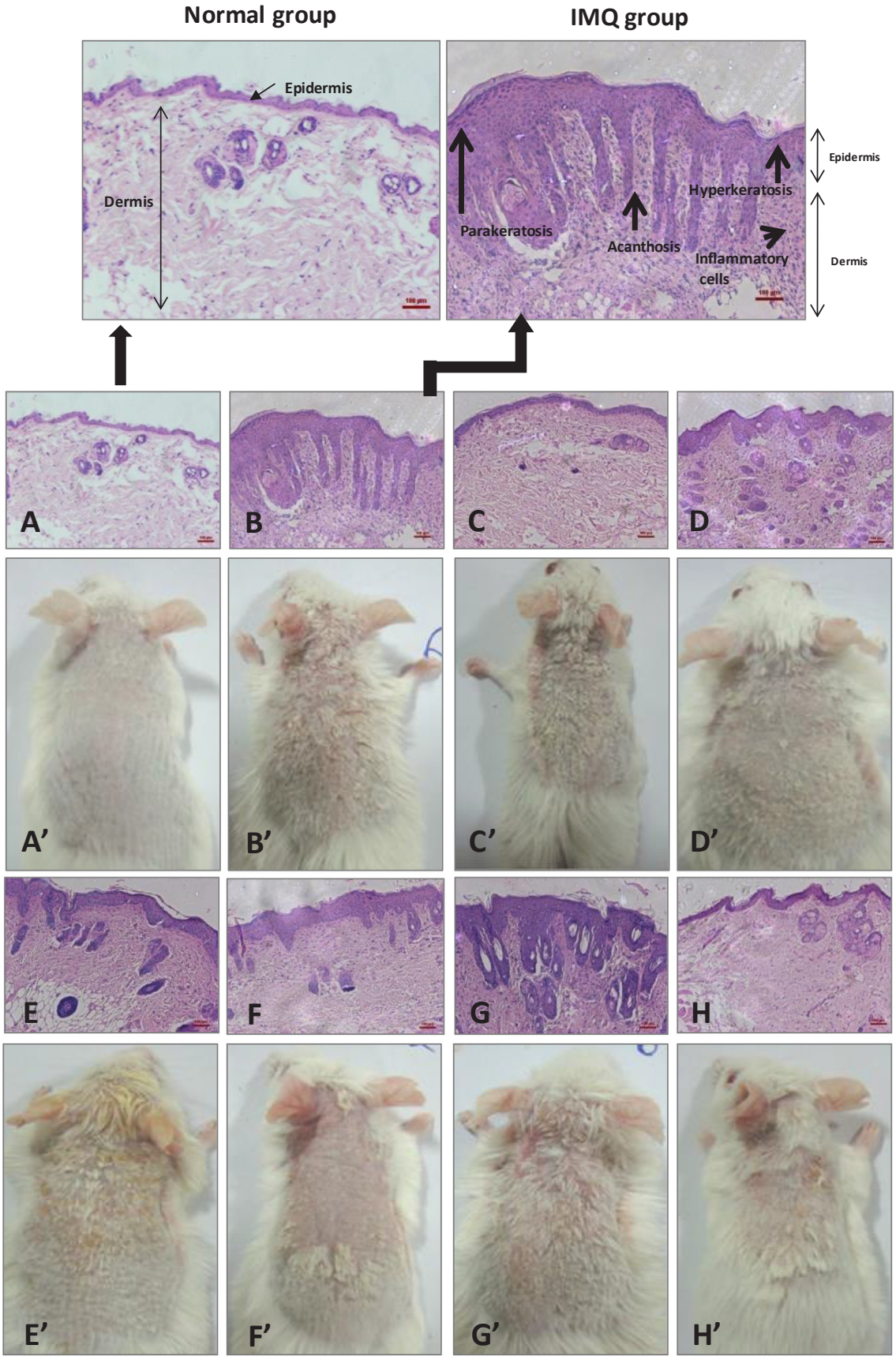

Fig. 6. Histopathological and phenotypic features of skin during IMQ induced psoriatic plaque model. (A & A') Normal group, (B & B') IMQ group, (C & C') Betamethasone group; (D & D') plain siTNF-α group; (E & E') blank P-G3 group; (F & F') P-G3 + siTNF-α group, (G & G') blank LPM group and (H & H') LPM + siTNF-α group.

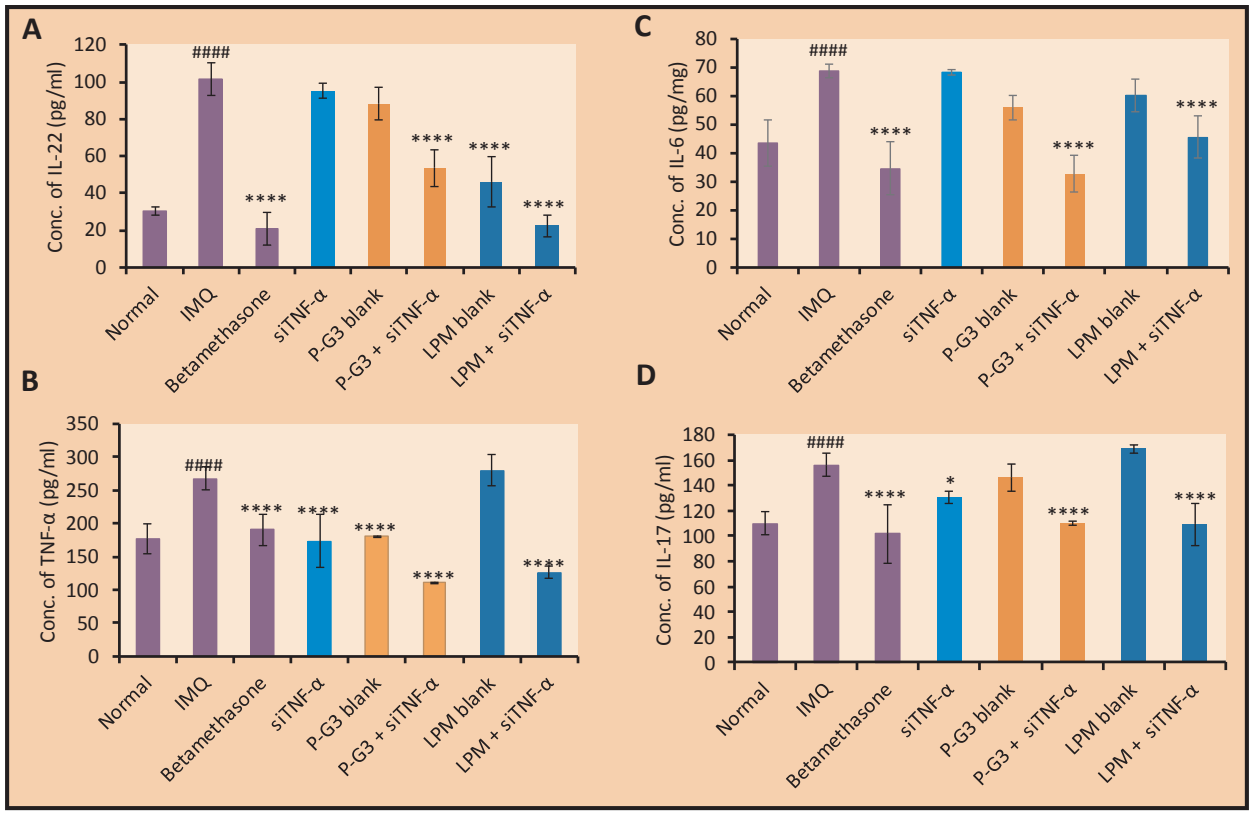

Fig. 7. Relative cytokine levels in skin homogenate of different groups during IMQ induced psoriatic plaque model. (A) Levels of IL-22, (B) levels of TNF-α, (C) levels of IL-6, (4) levels of IL-17. Values are expressed as mean ± SE, (n = 5). $^{*}P < 0.05$ (versus IMQ group), $^{****}P < 0.0001$ (versus IMQ group), $^{\#\#\#\#}P < 0.0001$ (versus normal group), $^{\theta\theta}P < 0.01$ (versus Betamethasone group), $^{\theta\theta\theta\theta}P < 0.0001$ (versus Betamethasone group).

retention of nuclei in stratum corneum (parakeratosis) and proliferation of the epidermis (acanthosis) with discreet chronic inflammatory infiltrates in the dermis. These features were markedly declined by treatment betamethasone, P-G3 + siTNF-α (dendriplex) and LPM + siTNF-α (lipoplex). However, improvement was not observed in blank siTNF-α group, blank P-G3 and blank LPM group in comparison to IMQ control.

3.6.4. Determination of cytokines levels

The skin homogenates obtained from mice skin of different control and treatment groups were analyzed for quantification of IL-22, TNF-α, IL-6 and IL-17 levels. In comparison to the normal group, IMQ group exhibited significant elevation of IL-22 (3.37 folds), TNF-α (1.52 folds), IL-6 (1.58 folds), and IL-17 (1.42 folds) levels indicating the induction of psoriasis (Fig. 7). In comparison to IMQ group, IL-22 levels were reduced to 4.90, 1.90 and 4.55 folds with betamethasone, P-G3 + siTNF-α and LPM + siTNF-α groups respectively (Fig. 7A).

TNF-α levels (Fig. 7B) were reduced to 1.40, 1.55, 2.43 and 2.11 folds with betamethasone, siTNF-α, P-G3 + siTNF-α and LPM + siTNF-α groups respectively when compared with IMQ group. Treatment groups P-G3 + siTNF-α and LPM + siTNF-α groups resulted in 1.73 and 1.51 folds reduction in TNF-α levels in comparison to betamethasone. In case of IL-6 levels (Fig. 7C), betamethasone, P-G3 + siTNF-α and LPM + siTNF-α resulted in 1.99, 2.09 and 1.50 folds reduction respectively in comparison to IMQ group. Similarly, IL-17 levels (Fig. 7D) were reduced to 1.53, 1.20, 1.42 and 1.43 folds with betamethasone, siTNF-α, P-G3 + siTNF-α and LPM + siTNF-α groups respectively when compared with IMQ group.

4. Discussion

In this study, dendriplex and lipoplex formulation of siTNF-α were prepared for topical application. The suitability of dendrimer as a carrier for topical delivery of siRNA was checked in comparison to DOTAP LPM. Formation of dendriplex and lipoplex was confirmed by gel electropherogram where the presence of uncomplexed siTNF-α was marked by sharp band and after complexation point no band was observed with increasing N/P ratio (for dendriplex) or molar ratio (for lipoplex). P-G3 dendriplex were formed at 2:1 N/P ratio whereas lipoplex were formed at 110:1 molar ratio. Zeta potential results also suggested sudden shift from negative to positive zeta potential near to complexation point due to charge neutralization followed by excess of carrier resulting positive zeta potential. Zeta potential for optimized dendriplex and lipoplex were 13.40 ± 4.84 mV and 29.96 ± 0.51 mV respectively. The particle size of optimized P-G3 dendriplex (99.80 ± 1.80 nm) was smaller than lipoplex (174.80 ± 0.80 nm) that can be explained by efficient charged interaction between P-G3 dendrimer and siTNF-α followed by condensation of dendriplex. Entrapment efficiency of siTNF-α in P-G3 dendriplex and lipoplex was 98.72 ± 2.02 and 94.99 ± 5.01% respectively. Both dendriplex and lipoplex were found to be stable in serum as well as in the presence of RNAse. *In vivo* efficacy of these formulations was determined using IMQ induced psoriatic plaque model where the developed lesions resembled the human psoriatic plaque. The phenotypic and histopathological features were improved in P-G3 dendriplex and lipoplex treated groups in comparison to IMQ groups. During psoriasis, the levels of cytokines IL-6, TNF-α, IL-17 and IL-22 are found to be elevated in IMQ group. P-G3 dendriplex resulted in 2.09 folds reduction while lipoplex resulted in 1.50 folds reduction in IL-6 levels in comparison to IMQ group. P-G3 dendriplex and lipoplex were found to be almost equally efficacious in the reduction of TNF-α (2.43 vs 2.41 folds, respectively) and IL-17 (1.42 vs 1.43, folds respectively) in comparison to IMQ group. As TNF-α is the primary cytokines that will be affected by siTNF-α, almost equal reduction in its level with both the carriers indicate suitability of

dendriplex for topical application. Though, lipoplex resulted in more reduction of IL-22 levels in comparison to IMQ group (4.55 folds with lipoplex vs 1.90 folds with dendriplex), IL-17 levels were reduced to 1.42 folds by both the carriers. Both the carriers were found to be safe for topical application as suggested by skin compliance data and hematological screening where difference between normal and formulation treated groups was insignificant.

5. Conclusion

Cationic liposomes for siRNA delivery (lipoplexes) were well established from long time. In this study, we compared the effectiveness of TNF-α siRNA loaded dendriplexes vs lipoplexes for management of psoriasis. From the above experimental results it was concluded that P-G3 dendrimers are equally efficacious to DOTAP LPM for topical delivery of TNF-α siRNA in psoriasis and they can be explored further for topical delivery of other genes.

Acknowledgements

This work is supported by Indo-Polish joint project under India-Polish Inter-Governmental, Science & Technology Cooperation programme (DST/INT/POL/P-12/2014).

Declaration of interest

The authors have no relevant affiliations or financial involvement with any organization or entity with a financial interest in or financial conflict with the subject matter or materials discussed in the manuscript. This includes employment, consultancies, honoraria, stock ownership or options, expert testimony, grants or patents received or pending, or royalties.

References

Zhou, Y., Zhang, C., Liang, W., 2014. Development of RNAi technology for targeted therapy—a track of siRNA based agents to RNAi therapeutics. J. Control. Release 193, 270–281.
Sokolova, V., Kovtun, A., Prymak, O., Meyer-Zaika, W., Kubareva, E.A., Romanova, E.A., et al., 2007. Functionalisation of calcium phosphate nanoparticles by oligonucleotides and their application for gene silencing. J. Mater. Chem. 17 (8), 721–727.
Pecot, C.V., Calin, G.A., Coleman, R.L., Lopez-Berestein, G., Sood, A.K., 2011. RNA interference in the clinic: challenges and future directions. Nat. Rev. Cancer 11 (1), 59–67.
Jain, A., Muntimadugu, E., Domb, A.J., Khan, W., 2014. Cationic polysaccharides in gene delivery. In: Cationic Polymers in Regenerative Medicine. Royal Society of Chemistry, pp. 228–248.
O'Mahony, A.M., Ogier, J., Desgranges, S., Cryan, J.F., Darcy, R., O'Driscoll, C.M., 2012. A click chemistry route to 2-functionalised PEGylated and cationic β-cyclodextrins: co-formulation opportunities for siRNA delivery. Org. Biomol. Chem. 10 (25), 4954–4960.
Moser, K., Kriwet, K., Naik, A., Kalia, Y.N., Guy, R.H., 2001. Passive skin penetration enhancement and its quantification in vitro. Eur. J. Pharm. Biopharm. 52 (2), 103–112.
Barry, B.W., 2001. Novel mechanisms and devices to enable successful transdermal drug delivery. Eur. J. Pharm. Sci. 14 (2), 101–114.
Pandi, P., Jain, A., Raju, S., Khan, W., 2017. Therapeutic approaches for the delivery of TNF-α siRNA. Therapeutic Delivery 8 (5), 343–355.
Akinc, A., Goldberg, M., Qin, J., Dorkin, J.R., Gamba-Vitalo, C., Maier, M., et al., 2009. Development of lipidoid–siRNA formulations for systemic delivery to the liver. Mol. Ther. 17 (5), 872–879.
Desai, P.R., Marepally, S., Patel, A.R., Voshavar, C., Chaudhuri, A., Singh, M., 2013. Topical delivery of anti-TNFα siRNA and capsaicin via novel lipid-polymer hybrid nanoparticles efficiently inhibits skin inflammation in vivo. J. Control. Release 170 (1), 51–63.
Doppalapudi, S., Shaheen, M., Khan, W., 2017. Development and in vitro assessment of psoralen and resveratrol co-loaded ultradeformable liposomes for the treatment of vitiligo. J. Photochem. Photobiol., B 174, 44–57.
Bulbake, U., Doppalapudi, S., Kommineni, N., Khan, W., 2017. Liposomal formulations in clinical use: an updated review. Pharmaceutics 9 (2), 12.
Uppuluri, S., Dvornic, P.R., Klimash, J.W., Carver, P.I., Tan, N.C., 1998. The properties of dendritic polymers I: generation 5 poly (amidoamine) dendrimers. DTIC Document.
Kang, H., DeLong, R., Fisher, M.H., Juliano, R.L., 2005. Tat-conjugated PAMAM dendrimers as delivery agents for antisense and siRNA oligonucleotides. Pharm. Res. 22 (12), 2099–2106.
A. Jain, H. Hosseinkhani, A.J. Domb, W. Khan, Cationic Polymers for the Delivery of Therapeutic Nucleotides. Polysaccharides: Bioactivity and Biotechnology, 2015, 1969–1990.
Ionov, M., Lazniewska, J., Dzmitruk, V., Halets, I., Loznikova, S., Novopashina, D., et al., 2015. Anticancer siRNA cocktails as a novel tool to treat cancer cells. Part (A). Mechanisms of interaction. Int. J. Pharm. 485 (1), 261–269.
Podesta, J.E., Kostarelos, K., 2009. Chapter seventeen-engineering cationic liposome: siRNA complexes for in vitro and in vivo delivery. Methods Enzymol. 464, 343–354.
Sato, Y., Hatakeyama, H., Sakurai, Y., Hyodo, M., Akita, H., Harashima, H., 2012. A pH-sensitive cationic lipid facilitates the delivery of liposomal siRNA and gene silencing activity in vitro and in vivo. J. Control. Release 163 (3), 267–276.
Jones, L.J., Yue, S.T., Cheung, C.-Y., Singer, V.L., 1998. RNA quantitation by fluorescence-based solution assay: RiboGreen reagent characterization. Anal. Biochem. 265 (2), 368–374.
Du, J., Sun, Y., Shi, Q.-S., Liu, P.-F., Zhu, M.-J., Wang, C.-H., et al., 2012. Biodegradable nanoparticles of mPEG-PLGA-PLL triblock copolymers as novel non-viral vectors for improving siRNA delivery and gene silencing. Int. J. Mol. Sci. 13 (1), 516–533.
Zhang, Y., Li, H., Sun, J., Gao, J., Liu, W., Li, B., et al., 2010. DC-Chol/DOPE cationic liposomes: a comparative study of the influence factors on plasmid pDNA and siRNA gene delivery. Int. J. Pharm. 390 (2), 198–207.
Kim, H.-K., Davaa, E., Myung, C.-S., Park, J.-S., 2010. Enhanced siRNA delivery using cationic liposomes with new polyarginine-conjugated PEG-lipid. Int. J. Pharm. 392 (1), 141–147.
Somiya, M., Yamaguchi, K., Liu, Q., Niimi, T., Maturana, A.D., Iijima, M., et al., 2015. One-step scalable preparation method for non-cationic liposomes with high siRNA content. Int. J. Pharm. 490 (1), 316–323.
Koide, H., Okamoto, A., Tsuchida, H., Ando, H., Ariizumi, S., Kiyokawa, C., et al., 2016. One-step encapsulation of siRNA between lipid-layers of multi-layer polycation liposomes by lipoplex freeze-thawing. J. Control. Release 228, 1–8.
Jain, A., Venkatesh, P., Bulbake, U., Doppalapudi, S., Rafeeqi, T.A., Godugu, C., et al., 2017. Liposphere mediated topical delivery of Thymoquinone in the treatment of psoriasis. Nanomed. Nanotechnol. Biol. Med. 13, 2251–2262.
Chen, H.-T., Neerman, M.F., Parrish, A.R., Simanek, E.E., 2004. Cytotoxicity, hemolysis, and acute in vivo toxicity of dendrimers based on melamine, candidate vehicles for drug delivery. J. Am. Chem. Soc. 126 (32), 10044–10048.
van der Fits, L., Mourits, S., Voerman, J.S., Kant, M., Boon, L., Laman, J.D., et al., 2009. Imiquimod-induced psoriasis-like skin inflammation in mice is mediated via the IL-23/IL-17 axis. J. Immunol. 182 (9), 5836–5845.
Jain, A., Doppalapudi, S., Domb, A.J., Khan, W., 2016. Tacrolimus and curcumin co-loaded liposphere gel: synergistic combination towards management of psoriasis. J. Control. Release 243, 132–145.
Sun, L., Liu, Z., Wang, L., Cun, D., Tong, H.H., Yan, R., et al., 2017. Enhanced topical penetration, system exposure and anti-psoriasis activity of two particle-sized, curcumin-loaded PLGA nanoparticles in hydrogel. J. Control. Release 254, 44–54.
Fadzil, M.A., Ihtatho, D., Affandi, A.M., Hussein, S., 2009. Area assessment of psoriasis lesions for PASI scoring. J. Med. Eng. Technol. 33 (6), 426–436.
De Rosa, G., Mignogna, C., 2007. The histopathology of psoriasis. Reumatismo 59 (1s), 46–48.
Doppalapudi, S., Jain, A., Chopra, D.K., Khan, W., 2017. Psoralen loaded liposomal nanocarriers for improved skin penetration and efficacy of topical PUVA in psoriasis. Eur. J. Pharm. Sci. 96, 515–529.
Tang, Y., Li, Y.-B., Wang, B., Lin, R.-Y., van Dongen, M., Zurcher, D.M., et al., 2012. Efficient in vitro siRNA delivery and intramuscular gene silencing using PEG-modified PAMAM dendrimers. Mol. Pharm. 9 (6), 1812–1821.